Magazine of Civil Engineering

ISSN 2712-8172

journal homepage: http://engstroy.spbstu.ru/

Research article

UDC 624.046.3

DOI: 10.34910/MCE.119.4

Numerical buckling calculation method for composite rods with semi-rigid ties

E.V. Popov ✉, ***B.V. Labudin***, ***A.Y. Konovalov***, ***A.V. Karelskiy***, ***V.V. Sopilov***, ***A.V. Bobyleva***, ***D.A. Stolypin***

Northern (Arctic) Federal University named after M.V. Lomonosov, Arkhangelsk, Russia

✉ *EPV1989@yandex.ru*

Keywords: composite structures, semi-rigid connections, buckling, numerical methods, nonlinear analysis, experimental study, shear stiffness

Abstract. Research object: composite centrally-compressed structures with semi-rigid nonlinearly deformable connections, which are put into operation at the very beginning of loading the element. Research goal: development of a numerical method for calculating the strength and stability of compressed composite rods, which takes into account the nonlinear deformation of shear bonds, the shear stiffness coefficient of which has the form of a functional dependence and is equal to the angle of inclination of the tangent drawn to the experimental load–strain curve (T–δ) at the point with a given shear force T. Methods: the method of solving the problem consists in dividing the component element into separate sections, compiling a system of equations describing the increment of contiguous fibers in the shear seams. The load is applied in steps, after the next step the total shear forces in the bonds are determined and the stiffness coefficients for the next calculation step are clarified; at each step, the system is "probing" for the possibility of loss of stability. The resulting value of the critical force is compared with the sum of all load steps applied at this stage of the calculation, the calculation stops when the specified calculation accuracy is reached. If necessary, to obtain the resulting values, the received forces in the bonds and the normal stresses in the branches of the component structure are summed up. Results: the calculation of a three-layer timber pillar is presented. The pillar is reinforced with side overlays fastened using nonlinear-compliant shear bonds. The results of linear and nonlinear calculations are compared for different values of the stiffness coefficient of the bonds. The possible calculation error with the normative value of the stiffness coefficient is established.

Funding: This research work was supported by the Northern (Arctic) Federal University named after M.V. Lomonosov, Arkhangelsk, Russian Federation.

Citation: Popov, E.V., Labudin, B.V., Konovalov, A.Y., Karelskiy, A.V., Sopilov, V.V., Bobyleva, A.V., Stolypin, D.A. Numerical buckling calculation method for composite rods with semi-rigid ties. Magazine of Civil Engineering. 2023. 119(3). Article no. 11904. DOI: 10.34910/MCE.119.4

1. Introduction

Timber and timber-composite products serve as the starting material for the manufacture of various building structures. This is because such structures have high architectural merit, are reliable, strong, durable and virtually light. They are economical, resistant to aggressive environments. In many countries of the world, there is a huge renewable raw material base for the manufacture of such structures. The use of timber in the construction of public, industrial, agricultural, and multi-storey residential and warehouse frame buildings is becoming increasingly popular. The main load-bearing elements of such buildings are, as a rule, timber or timber composite columns, the calculation and design of which are discussed in a number of works by domestic and foreign scientists.

Paper [1] presents the results of a monitoring case study on a tall timber–hybrid building in Switzerland, a 15 storey, and 60 m high office building completed in 2019. A fibre–optic measuring system showed an increase of the deformation with increasing load during the construction phase of highly stressed spruce–GLT and beech–LVL columns. However, the highest strain values were not reported in the columns themselves but at the ceiling transitions and in the area near their supports.

In [2, 3] the strength and stability of timber columns with steel cores of various configurations under central compression is studied. In studies [4, 5] are considered columns with a timber core, covered with a steel shell of round and square cross-section. Article [6] steel-wood-concrete columns with a double steel shell and various configurations of the location of the placeholder relative to the cross section of the element are investigated.

A steel–timber axial compressed composite (STC) column made of H-shaped steel and glulam is proposed in paper [7].

A novel L-shaped steel-timber composites column, fabricated using STC (L-STC), which are used in the construction of large-span structures and multistory buildings under concentric loading, was proposed in paper [8].

The objective of study [9] is to establish a theoretical calculation model for this type of retrofitted splice columns. Firstly, a theoretical model for the axial compressive strength of splice columns retrofitted with a steel jacket is proposed considering the contact stresses at a splice joint and the relevant stability theory. Secondly, the buckling modes of splice columns and the actual stress distributions at the splice joints are thoroughly investigated. Finally, the theoretical model is confirmed by the experimental data and the results of finite element analysis with different splice parameters.

In [10] various performance improvement techniques have been used for enhancing the strength parameters in long columns made from a timber specie (Poplar) found in abundance in the Kashmir region of India. Poplar used in the cross-laminated form with different binding/wrapping techniques viz. bolted, wrapped cold steel, single helix carbon fiber reinforced polymer (FRP), and double helix carbon FRP wrapping, have been fabricated and tested.

The work [11] investigated the different axial compression behaviors of cross–laminated timber columns (CLTCs) and control glued–laminated timber columns (GLTCs). The average compression modulus of elasticity (MOE) and strength values of the CLTCs were lower than those of the control GLTCs and appeared to be dependent on the area ratio in the axial direction. The column length had different effects on the compression behaviors of CLTCs and GLTCs, and compared with the GLTCs, the CLTCs exhibited enhanced ductility and energy absorption properties due to the cross–lamination.

A number of new design developments [12, 13] made it possible to design columns with a rigid joint in the reference section.

Despite extensive research in the field of calculations, design and testing of component timber and timber composite columns, all of them apply only to such structures with rigid shear bonds between the constituent layers. There are no studies on the assessment of the sustainability of such structures in the presence of nonlinear compliance of discrete bonds. In some cases, for example, in centrally compressed two-layer component columns, shear bonds are put into operation only at the moment of loss of stability, which is due to the appearance of a bending moment from the action of a longitudinal compressive force during creep. For such elements, the stability calculation can be carried out taking into account the initial stiffness modulus of compliant joints. For the three-layer component elements presented in Fig. 1, a characteristic feature will be the occurrence of forces in shear bonds already at the very beginning of loading, since due to the work of shear bonds, the load is redistributed between the central and peripheral layers.

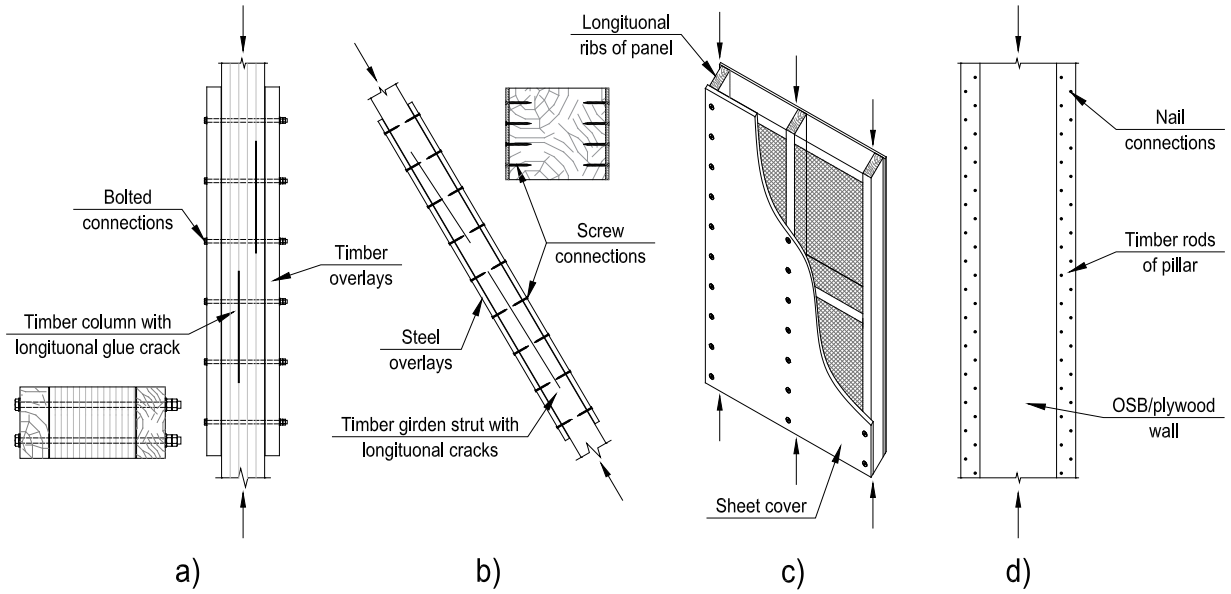

Figure 1. Component timber composite elements: *a* – glued timber column with longitudinal cracks reinforced timber overlays with bolted connections; *b* – timber girder strut reinforced steel overlays with screw connections; *c* – wall panel with sheet cover included in the joint work with ribs; *d* – I-section pillar with timber chords and sheet material wall (plywood, OSB, etc.).

At the moment of loss of stability, the shear bonds from the concave side of the element will experience additional loading, the stiffness modulus of the bonds will be determined by the slope of the tangent to the "load-strain" dependence (Fig. 2). Shear bonds located on the curved side of the element will experience unloading according to the linear law $\left(c = \mathrm{tg}\beta\right)$, as a result of which their actual stiffness modulus will be equal to their initial stiffness modulus $\left(c = \mathrm{tg}\alpha\right)$. The more significant the characteristic of nonlinearity for compliant joints, the more this factor will affect the stability of the component element. The method given in [14] for calculating component rod elements on compliant bonds involves the use of a linear stiffness coefficient k_u, which does not allow taking into account the real nature of the deformation of the joints, and, as a result, adequately assessing the stability reserves of such structures.

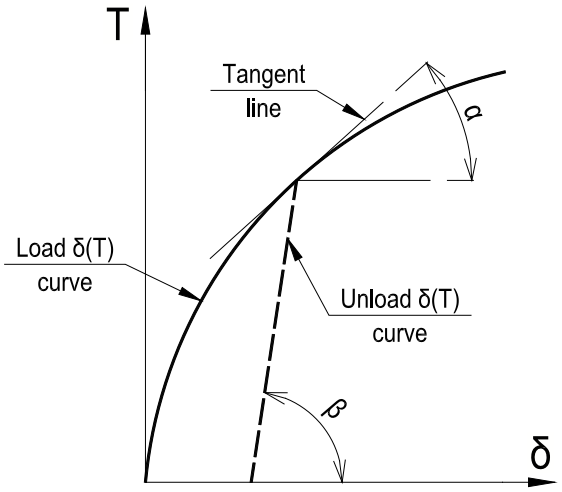

Figure 2. Scheme for determining the joint stiffness modulus for a given force during additional loading and unloading: α – angle of inclination of the tangent line at a point at actual stress values; β – is the same, at the beginning of loading.

The research object is build–up centric–compressed timber pillars. The subject of research is nonlinear dependence "load–shear" of ties and stability of such structures. The purpose of the article is to design the mathematical step method for stability estimation, which considers nonlinear deformability of shear ties. The task of researches is to calculate a three–layer build–up timber rod critical force according to the developed mathematical model, and to compare the exact and approximate critical force calculations of such structure with the assumption of different approaches in determining of elastic modulus of the ties.

2. Methods

For most types of shear bonds: nogs [15], bolts [16], MTP [17], claw connectors [18], screws [19], brackets [20] and others are characterized by nonlinear dependence between the load and the deformation of the joint. Thus, for component columns with nonlinearly deformable compliant joints, it is necessary to take into account the change in the stiffness of shear bonds depending on the forces acting in them, that is, the stiffness coefficient of each bond should be considered as a function [21]:

$$c = c\left(T_c\right), \tag{1}$$

where c is shear stiffness of a single joint; T_c is force applied to the joint.

The common chain for the such task numerical solution is presented in the form of a block scheme in Fig. 3.

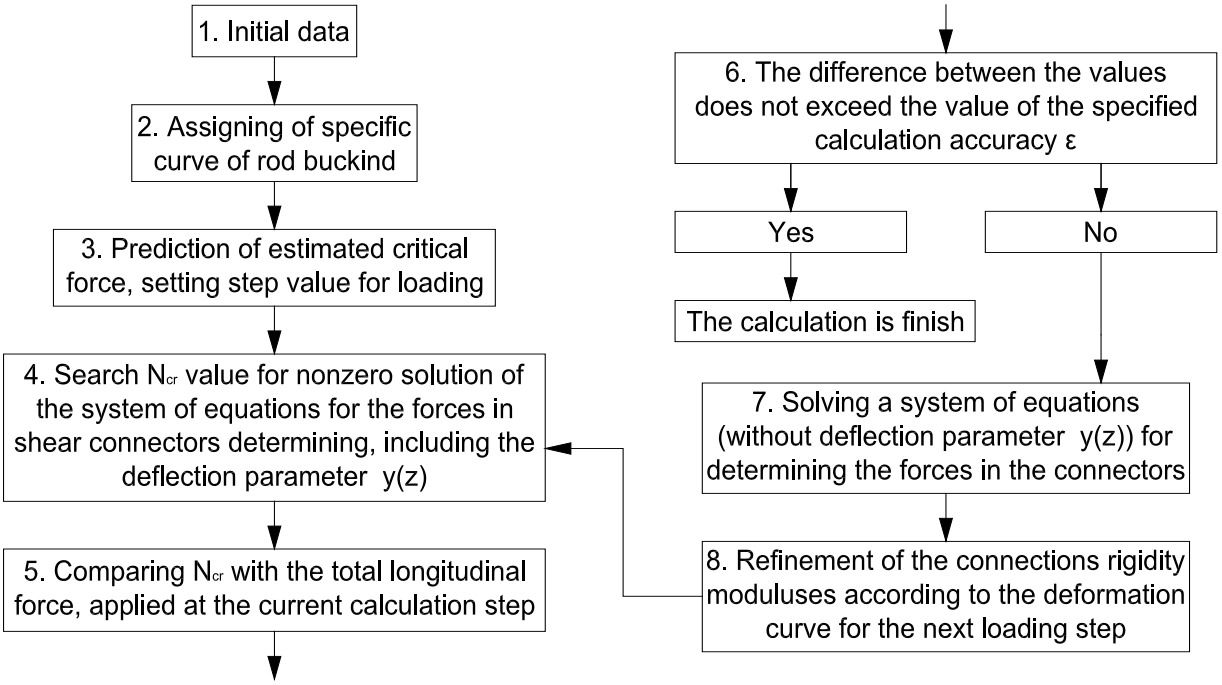

Figure 3. Block scheme of numerical solution.

The composite element, which is shown in Fig. 4, can be considered. Under the action of a longitudinal force applied to the central element, shear forces arise in shear bonds $T_{1,i}$ and $T_{2,i}$, where the first index means the seam number, and the second – the number of the discrete bond. To construct an algorithm, we consider a symmetrical case with respect to the middle of the height for a three-layer component element, the outer layers of which are not obstructed by mutual displacements along the ends. The interconnection of the layers is carried out due to flexible shear bonds, located, in general, with a variable step, but symmetrically with respect to the section with zero shear deformations and the center of gravity of the section of the middle element.

The i-th section of the element can be considered, limited by i-th and $i+1$-th connectors. The increment of the concentrated shear along the length of the allocated site will be equal to the difference in shears i-th and $i+1$-th bonds on a section of length l_i and is described by the system of equations:

$$\begin{cases} \Gamma_{1,i+1}-\Gamma_{1,i}=\dfrac{T_{1,i+1}}{c_{1,i+1}}-\dfrac{T_{1,i}}{c_{1,i}}= \\ =\Delta_{11,i}l_i\sum\limits_{k=1}^{i}T_{1,k}+\Delta_{12,i}l_i\sum\limits_{k=1}^{i}T_{2,k}+\int\limits_{0}^{l_i}\Delta_{10,i}\left(z_i\right)dz_i; \\ \Gamma_{2,i+1}-\Gamma_{2,i}=\dfrac{T_{2,i+1}}{c_{2,i+1}}-\dfrac{T_{2,i}}{c_{2,i}}= \\ =\Delta_{21,i}l_i\sum\limits_{k=1}^{i}T_{1,k}+\Delta_{22,i}l_i\sum\limits_{k=1}^{i}T_{2,k}+\int\limits_{0}^{l_i}\Delta_{20,i}\left(z_i\right)dz_i, \end{cases} \quad (2)$$

where $\Gamma_{1,i}$, $\Gamma_{2,i}$ are concentrated shifts of i-th bond of 1st and 2nd seams, respectively; $c_{1,i}$, $c_{2,i}$ are stiffness coefficient of i-th bond of 1st and 2nd seams; z_i is the coordinate measured by length i-th section; $\Delta_{11,i}$, $\Delta_{12,i}$, $\Delta_{22,i}$ are coefficients of equations that take into account the amount of shear from unknown shear forces $T_{1,i}$, $T_{2,i}$; $\Delta_{10,i}$, $\Delta_{20,i}$ are load functions that take into account the impact on shear of external loads applied to the structure.

$$\begin{aligned} \Delta_{11}&=\frac{1}{E_1^zF_1}+\frac{1}{E_2^zF_2}+\frac{w_1^2}{\sum E^zI^y}; \\ \Delta_{12}&=\Delta_{21}=\frac{w_1w_2}{\sum E^zI^y}-\frac{1}{E_2^zF_2}; \\ \Delta_{22}&=\frac{1}{E_2^zF_2}+\frac{1}{E_3^zF_3}+\frac{w_2^2}{\sum E^zI^y}; \end{aligned} \quad (3)$$

$$\begin{aligned} \Delta_{10,i}&=\frac{N_2}{E_2^zF_2}-\frac{N_1}{E_1^zF_1}-\frac{M_{0,i}\left(z_i\right)\cdot w_1}{\sum E^zI^y}; \\ \Delta_{20,i}&=\frac{N_3}{E_3^zF_3}-\frac{N_2}{E_2^zF_2}-\frac{M_{0,i}\left(z_i\right)\cdot w_2}{\sum E^zI^y}, \end{aligned} \quad (4)$$

where F_1, F_2, F_3, E_1, E_2, E_3 are cross-sectional areas and elastic modulus of the branch material of a component column; N_1, N_2, N_3 are longitudinal forces in the branches; w_i are distances between centers of gravity of branches; $\sum El$ is the sum of the stiffness of the layers: $\sum E^zI^y=E_1^zI_1++E_2^zI_2+E_3^zI_3$; $M_{0,i}\left(z_i\right)$ is distribution function of the bending moment within the i-th section.

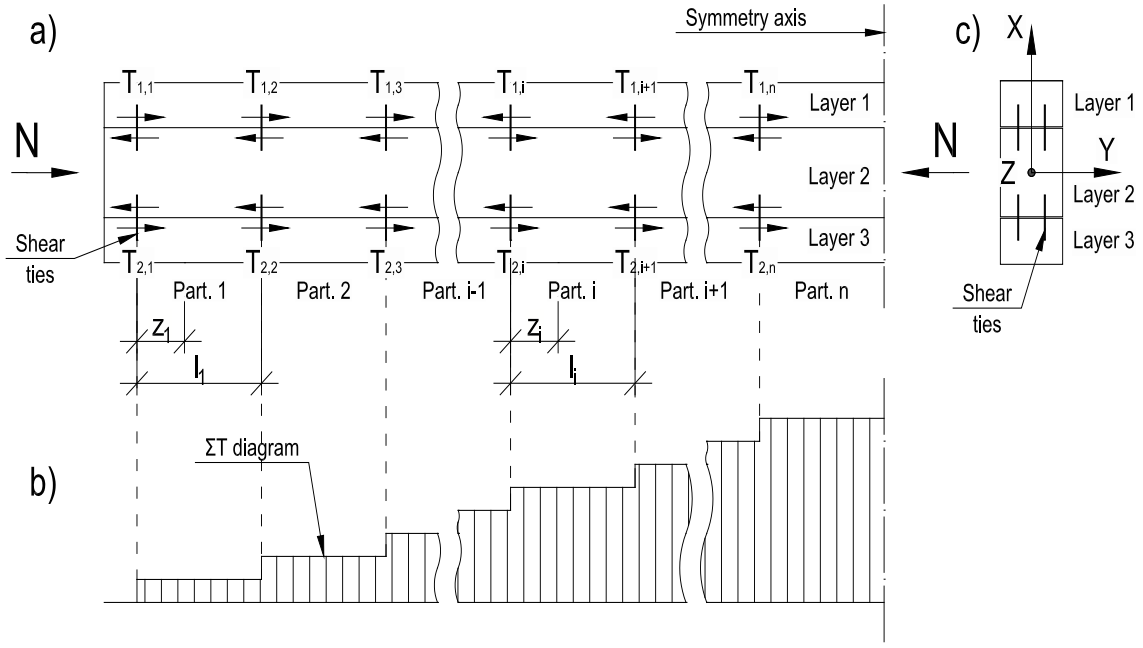

Figure 4. Scheme of a compressed composite pressed rod with discrete shear connections: a – numeration of bonds and sections; b – scheme of resulting shear forces in discrete connections diagram; c – composite rod cross-section; N – compressive force; T – shear forces in discrete connectors; X, Y, Z – coordinate axes.

Composing expressions (2) for each section of length l_i, a system of equations can be obtained to determine the shear forces in each connector:

$$\begin{cases} \dfrac{T_{j,2}}{c_{j,2}} - \dfrac{T_{j,1}}{c_{j,1}} = \Delta_{j1,1} \cdot l_1 \cdot T_{1,1} + \Delta_{j2,1} \cdot l_1 \cdot T_{2,1} + \int\limits_0^{l_1} \Delta_{j0,1}(z_1)\, dz_1 \\ \ldots \\ \dfrac{T_{j,i+1}}{c_{j,i+1}} - \dfrac{T_{j,i}}{c_{j,i}} = \Delta_{j1,i} \cdot l_i \cdot \sum\limits_{k=1}^{i} T_{1,k} + \Delta_{j2,i} \cdot l_i \cdot \sum\limits_{k=1}^{i} T_{2,k} + \int\limits_0^{l_i} \Delta_{j0,i}(z_1)\, dz_i, \\ \ldots \\ 0 - \dfrac{T_{j,n}}{c_{j,n}} = \Delta_{j2,n} \cdot l_n \cdot \sum\limits_{k=1}^{n} T_{1,k} + \Delta_{22,i} \cdot l_n \cdot \sum\limits_{k=1}^{i} T_{2,k} + \int\limits_0^{l_i} \Delta_{j0,n}(z_1)\, dz_n \end{cases} \quad (5)$$

where j is seam number $(j = 1,\ 2)$.

The index after the comma of the coefficients at unknown and free members means that in some cases they can be variable in the length of the element and be determined for each section (for example, in the case of a variable cross section or the presence of local defects in the reinforced structure).

A system with nonlinear elastic shear bonds is characterized by an uneven decrease in the modulus of stiffness [21, 22]; as a result, the calculation must be carried out by the step method. The total number of steps of the nonlinear calculation is denoted as $\sum m$, where m is step number $(m = 1,\ 2,\ 3 ... \sum m)$. We denote by ΔN_m the value of the step of application of the external load at the m-th calculation step.

The system of equations (5) for determining the forces at the m-th calculation step in shear bonds can be represented in matrix form:

$$X_m = A_m^{-1} \cdot B_m, \quad (6)$$

where X_m is the desired matrix of unknown shear forces $T_{1,i}$, $T_{2,i}$, A_m is matrix composed of coefficients at unknown shear forces (formulas (3)); B_m is matrix composed of free members, obtained by integrating expressions (4).

The index "m" in the designations given in formula (6) means that the elastic characteristics of materials at each calculation step can also be refined (when calculating taking into account the physical nonlinearity of materials).

$$A_m = \begin{bmatrix}
\frac{1}{c_{1,1}}+\Delta_{11,1}l_1 & -\frac{1}{c_{1,2}} & \dots & 0 & \dots & 0 & \Delta_{1,2}l_1 & 0 & \dots & 0 & \dots & 0 \\
\Delta_{11,1}l_2 & \frac{1}{c_{1,2}}+\Delta_{11,1}l_2 & \dots & 0 & \dots & 0 & \Delta_{12,2}l_2 & \Delta_{12,2}l_2 & \dots & 0 & \dots & 0 \\
 & & & & & \dots & \dots & & & & & \\
\Delta_{11,i}l_i & \Delta_{11,i}l_i & \dots & \frac{1}{c_{1i}}+\Delta_{11,i}l_i & \dots & 0 & \Delta_{12,i}l_i & \Delta_{12,i}l_i & \dots & \Delta_{12,i}l_i & \dots & 0 \\
 & & & & & \dots & \dots & & & & & \\
\Delta_{11,n}l_n & \Delta_{11,n}l_n & \dots & \Delta_{11,n}l_n & \dots & \frac{1}{c_{1,n}}+\Delta_{11,n}l_n & \Delta_{12,n}l_n & \Delta_{12,n}l_n & \dots & \Delta_{12,n}l_n & \dots & \Delta_{12,n}l_n \\
\Delta_{21,1}l_1 & 0 & \dots & 0 & \dots & 0 & \frac{1}{c_{2,1}}+\Delta_{22,2}l_1 & -\frac{1}{c_{2,2}} & \dots & 0 & \dots & 0 \\
\Delta_{21,1}l_2 & \Delta_{2,1}l_2 & \dots & 0 & \dots & 0 & 0 & \frac{1}{c_{2,2}}+\Delta_{22,2}l_2 & \dots & 0 & \dots & 0 \\
 & & & & & \dots & \dots & & & & & 0 \\
\Delta_{21,i}l_i & \Delta_{21,i}l_i & \dots & 0 & \dots & 0 & \Delta_{22,i}l_i & \Delta_{22,i}l_i & \dots & \frac{1}{c_{2,i}}+\Delta_{22,i}l_i & \dots & 0 \\
 & & & & & \dots & \dots & & & & & \\
\Delta_{21,1}l_n & \Delta_{21,1}l_n & \dots & \Delta_{21,1}l_n & \dots & 0 & \Delta_{22,n}l_2 & \Delta_{22,n}l_2 & \dots & \Delta_{22,n}l_2 & \dots & \frac{1}{c_{2,n}}+\Delta_{22,n}l_n
\end{bmatrix}; \quad (7)$$

$$B_m = \begin{bmatrix}
\dots \\
\dots \\
\dots \\
-\int_0^{l_i}\left(\frac{N_2}{E_2F_2}-\frac{N_1}{E_1F_1}-\frac{M_{0,i}w_1}{\sum EI}\right)dz_i \\
\dots \\
-\int_0^{l_n}\left(\frac{N_2}{E_2F_2}-\frac{N_1}{E_1F_1}-\frac{M_{0,n}w_1}{\sum EI}\right)dz_n \\
\dots \\
\dots \\
\dots \\
-\int_0^{l_i}\left(\frac{N_3}{E_3F_3}-\frac{N_2}{E_2F_2}-\frac{M_{0,i}w_2}{\sum EI}\right)dz_i \\
\dots \\
-\int_0^{l_n}\left(\frac{N_3}{E_3F_3}-\frac{N_2}{E_2F_2}-\frac{M_{0,n}w_2}{\sum EI}\right)dz_n
\end{bmatrix}; \quad X_m = \begin{bmatrix}
T_{1,1} \\
\dots \\
T_{1,2} \\
\dots \\
T_{1,i} \\
\dots \\
T_{1,n} \\
T_{2,1} \\
T_{2,2} \\
\dots \\
T_{2,i} \\
\dots \\
T_{2,n}
\end{bmatrix}. \quad (8)$$

At the calculation stage m the resulting force vector in the bonds can be represented as the sum of the required shear force vectors X_m at all previous and current calculation steps:

$$\vec{T}_{i,j} = \sum_{k=1}^{m} \vec{X}_k.$$

As the column is loaded, the forces in the bonds will increase, in the general case (with a decrease in the degree of loading of the derivative of the function describing the deformation of the bonds from the shear force T_c) the stiffness modulus of the bonds, which will cause to less in the stiffness of the component element as a whole. Therefore, it is impossible to determine in advance which stiffness value for each bond will correspond to the moment when the compressive load reaches a critical value.

At the moment of buckling, the centrally compressed rod will deviate from the initial rectilinear position, in addition to the longitudinal force, a bending moment will appear due to eccentricity:

$$M_0(z_i) = \sum N \cdot y(z_i), \tag{9}$$

whose meaning is unknown. Thus, one more equation will be added to the system of equations for determining shear deformations in the seams, for determining the deflection:

$$\sum EI \cdot y'' = \sum N \cdot y - w_1 \sum T_{1,\ldots} - w_2 \sum T_{2,\ldots}, \tag{10}$$

Under the action of an external load only on the middle element $(N_1 = N_3 = 0)$, the system of equations (5), with consideration of the moment from deflection during buckling, will take the form:

$$\begin{cases} \dfrac{T_{j,2}}{c_{j,2}} - \dfrac{T_{j,1}}{c_{j,1}} = \Delta_{1j,1} \cdot l_1 \cdot T_{1,1} + \\ + \Delta_{2j,1} \cdot l_1 \cdot T_{2,1} \pm \dfrac{N_2}{E_2 \cdot F_2} - \int\limits_0^{l_1} \dfrac{N_2 \cdot y(z_1) \cdot w_j}{\sum EI} dz_1; \\ \ldots \\ \dfrac{T_{j,i+1}}{c_{j,i+1}} - \dfrac{T_{j,i}}{c_{j,i}} = \Delta_{1j,i} \cdot l_i \cdot \sum\limits_{k=1}^{i} T_{1,k} + \\ + \Delta_{j2,i} \cdot l_i \cdot \sum\limits_{k=1}^{i} T_{2,k} \pm \dfrac{N_2}{E_2 \cdot F_2} - \int\limits_0^{l_i} \dfrac{N_2 \cdot y\left(\sum\limits_{k=1}^{i-1} l_k + z_i\right) \cdot w_j}{\sum EI} dz_i; \\ \ldots \\ 0 - \dfrac{T_{j,n}}{c_{j,n}} = \Delta_{1j,n} \cdot l_n \cdot \sum\limits_{k=1}^{n} T_{1,k} + \\ + \Delta_{2j,n} \cdot l_n \cdot \sum\limits_{k=1}^{n} T_{2,k} \pm \dfrac{N_2}{E_2 \cdot F_2} - \int\limits_0^{l_n} \dfrac{N_2 \cdot y\left(\sum\limits_{k=1}^{n-1} l_k + z_i\right) \cdot w_j}{\sum EI} dz_n; \\ (j = 1,2) \\ y''(z_1) \cdot \sum EI = \sum N \cdot y(z_1) - w_1 T_{1,1} - w_2 T_{2,1}; \\ \ldots \\ y''\left(\sum\limits_{k=1}^{n-1} l_k + z_n\right) \cdot \sum EI = \\ = N_2 \cdot y\left(\sum\limits_{k=1}^{n-1} l_k + z_n\right) - w_1 \sum\limits_{k=1}^{n-1} T_{1,k} - w_2 \sum\limits_{k=1}^{n-1} T_{2,k} \end{cases} \tag{11}$$

For some values of the longitudinal force $N_{cr} = N_2$ homogeneous system of equations obtained from (5) will have nonzero solutions. These values will correspond to the critical forces for many different forms of loss of stability. To determine N_{cr}, it is necessary to solve the equation:

$$\det|A| = 0. \tag{12}$$

where A is matrix consisting of the coefficients at unknowns of the homogeneous system of equations obtained from (11).

The calculation should be carried out by the method of successive approximations, in the following order (the order is considered for the m-th calculation step):

– given the value of the longitudinal force, the total shear forces in the bonds at the m-th step are determined. Based on these values, the tangent-modulus stiffness coefficients of joints located on the concave side of a compressed rod that loses stability are calculated by the formula:

$$c_i\left(T_i\right) = \frac{dT_i}{d\delta_i}, \tag{13}$$

where T_i is shear force attributable to the i-th bond; δ_i is the value of deformation of the i-th bond at a given load T_i, determined by the approximating function of the experimental curve of the deformation of the joint.

The stiffness coefficients of the bonds located in the opposite seam of the component rod are taken equal to the initial stiffness modulus, because they are experiencing unloading:

– the critical force is determined by solving the transcendental equation (12), the obtained value of the critical longitudinal force is compared with the total longitudinal force applied at the m-th calculation step:

$$\Delta = \frac{\left|\sum_{k=1}^{m} \Delta N_k - N_{cr}\right|}{N_{cr}} \le \varepsilon. \tag{14}$$

If the difference between the values does not exceed the value of the specified calculation accuracy ε, then the calculation is terminated, the value of the critical force is taken to be the value that is the solution of equation (12). If (14) is not fulfilled, the calculation continues in the same way for the step m+1, m+2, etc. until condition (14) is met.

As an example, consider a component timber pillar reinforced on both sides with timber overlays (Fig. 5,a). There are no obstacles to mutual shear at the end faces of the column. The column and overlays are made of pine wood of strength class C22 with an elastic modulus $E_{0.05}$ = 6.7 GPa. The branches of the component column are interconnected by steel bolted joints and toothed connectors. To obtain characteristics of the stiffness of the joints tests of samples of joints for intermediate shear were performed. The deformation of the joints occurs according to a nonlinear law, i.e. the stiffness parameter of the joints is expressed by the dependence $c = c\left(T_c\right)$ (Fig. 5, c). The behavior of timber is assumed linearly elastic. The following parameters are accepted as initial data: column height: H = 5 m, column cross-sectional dimensions 200×150 mm, overlays – 50×150 mm. Shear bonds spacing is $S_1 = S_2 = S_3 = S_4 = S_5 = 0.5$ m. Column loaded with longitudinal force N, transmitted to the column central middle element. It is necessary to define the value of the critical force.

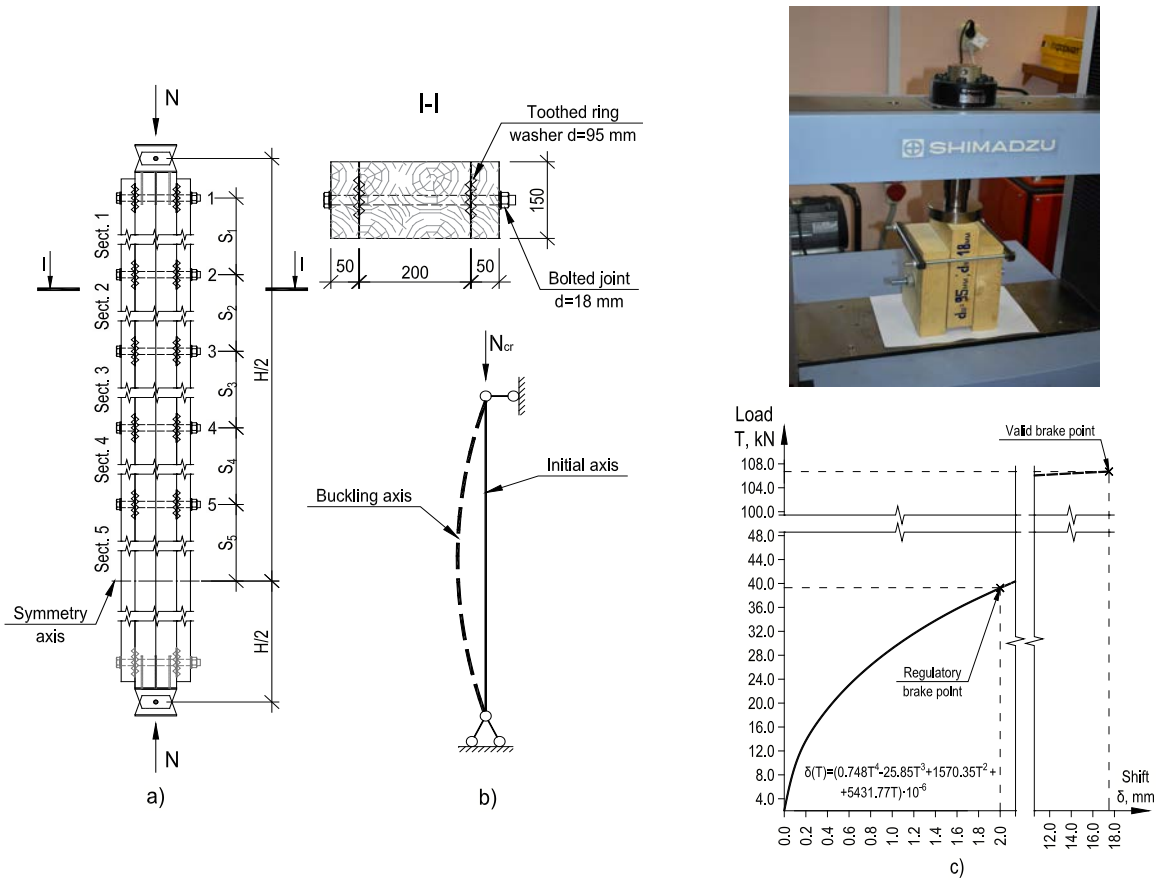

Figure 5. The component column on compliant bonds: *a* – column scheme; *b* – form of loss of stability with hinged fixing of ends; *c* – testing of samples on a hydraulic press Shimadzu and load-shift diagram (*T*–δ) for a single bond with longitudinal shift (for 1 seam).

Loading is performed by the step method, the value of the loading step is taken equal to ΔN = 50 kN. Determination of forces in shear bonds at each calculation step is made by solving the equation (6). According to the resulting forces in the shear bonds obtained at the previous step, according to expression (13), the stiffness coefficients of the bonds are assigned for the next calculation step. In addition, at each step, the system is "probing" for the possibility of loss of stability, for which equation (12) is solved and the results are compared according to expression (14). Taking into account the conditions of fixing, the buckling deflection function for the considered pillar can be represented by an affine curve:

$$y = \alpha \cdot \sin \frac{n\pi z}{H}, \tag{15}$$

where α is dimensionless parameter that determines the maximum deflection amplitude; n is number of pillar bending half-waves (in the considered case, the smallest critical force corresponds to n = 1); z is element height coordinate; H is full pillar height.

Since the shape of the pillar bend depends only on a single parameter – α, then in the case under consideration, the number of equations of system (11) can be reduced from 15 to 11 pcs. (as unknown parameters, the forces in the shear bonds $T_{j,i}$ and the parameter α). The matrix of coefficients for unknowns, compiled for a homogeneous system of equations, will have the form:

$$A=\begin{bmatrix}
\frac{1}{c_{1,1}}+\Delta_{1,1}l_1 & \frac{-1}{c_{1,2}} & 0 & 0 & 0 & \Delta_{2,1}l_1 & 0 & 0 & 0 & 0 & \Delta_{1,1y}\\
\Delta_{1,1}l_2 & \frac{1}{c_{1,2}}+\Delta_{1,1}l_2 & \frac{1}{c_{1,3}} & 0 & 0 & \Delta_{2,1}l_2 & \Delta_{2,1}l_2 & 0 & 0 & 0 & \Delta_{1,2y}\\
\Delta_{1,1}l_3 & \Delta_{1,1}l_3 & \frac{1}{c_{1,3}}+\Delta_{1,1}l_3 & \frac{1}{c_{1,4}} & 0 & \Delta_{2,1}l_3 & \Delta_{2,1}l_3 & \Delta_{2,1}l_3 & 0 & 0 & \Delta_{1,3y}\\
\Delta_{1,1}l_4 & \Delta_{1,1}l_4 & \Delta_{1,1}l_4 & \frac{1}{c_{1,4}}+\Delta_{1,1}l_4 & \frac{1}{c_{1,5}} & \Delta_{2,1}l_4 & \Delta_{2,1}l_4 & \Delta_{2,1}l_4 & \Delta_{2,1}l_4 & 0 & \Delta_{1,4y}\\
\Delta_{1,1}l_5 & \Delta_{1,1}l_5 & \Delta_{1,1}l_5 & \Delta_{1,1}l_5 & \frac{1}{c_{1,5}}+\Delta_{1,1}l_5 & \Delta_{2,1}l_5 & \Delta_{2,1}l_5 & \Delta_{2,1}l_5 & \Delta_{2,1}l_5 & \Delta_{2,1}l_5 & \Delta_{1,5y}\\
\Delta_{2,1}l_1 & 0 & 0 & 0 & 0 & \frac{1}{c_{2,1}}+\Delta_{2,1}l_1 & \frac{-1}{c_{2,1}} & 0 & 0 & 0 & \Delta_{2,1y}\\
\Delta_{2,1}l_2 & \Delta_{2,1}l_2 & 0 & 0 & 0 & \Delta_{2,2}l_2 & \frac{1}{c_{2,2}}+\Delta_{2,2}l_2 & \frac{-1}{c_{2,2}} & 0 & 0 & \Delta_{2,2y}\\
\Delta_{2,1}l_3 & \Delta_{2,1}l_3 & \Delta_{2,1}l_3 & 0 & 0 & \Delta_{2,2}l_3 & \Delta_{2,2}l_3 & \frac{1}{c_{2,3}}+\Delta_{2,3}l_3 & \frac{-1}{c_{2,4}} & 0 & \Delta_{2,3y}\\
\Delta_{2,1}l_4 & \Delta_{2,1}l_4 & \Delta_{2,1}l_4 & \Delta_{2,1}l_4 & 0 & \Delta_{2,2}l_3 & \Delta_{2,2}l_3 & \Delta_{2,2}l_3 & \frac{1}{c_{2,4}}+\Delta_{2,4}l_4 & \frac{-1}{c_{2,5}} & \Delta_{2,4y}\\
\Delta_{2,1}l_5 & \Delta_{2,1}l_5 & \Delta_{2,1}l_5 & \Delta_{2,1}l_5 & \Delta_{2,1}l_5 & \Delta_{2,2}l_3 & \Delta_{2,2}l_3 & \Delta_{2,2}l_3 & \Delta_{2,2}l_3 & \frac{1}{c_{2,5}}+\Delta_{2,5}l_5 & \Delta_{2,5y}\\
-w_1 & -w_1 & -w_1 & -w_1 & -w_1 & -w_2 & -w_2 & -w_2 & -w_2 & -w_2 & \Delta_{yy}
\end{bmatrix} \quad (16)$$

where Δ_{iy}, $\Delta_{i'y}$ are coefficients that considering the impact of the moment from the longitudinal force on the value of the shear forces in the seams, determined by the formulas (17); Δ_{yy} is multiplier at unknown parameter α, obtained from expression (10) subject to the accepted deformation curve (15), determined by the formula (18).

$$\Delta_{1,iy}=\frac{1}{\sum EI}\int_0^{l_i} N_2 w_1 \sin\left(\frac{\sum_{k=1}^{i-1} l_k + z_i}{H}\right) dz_i;$$
$$\Delta_{2,iy}=\frac{1}{\sum EI}\int_0^{l_i} N_2 w_2 \sin\left(\frac{\sum_{k=1}^{i-1} l_k + z_i}{H}\right) dz_i; \quad (17)$$

$$\Delta_{yy}=\frac{1}{H^2}\pi^2\sum EI\sin\left(\frac{\pi}{2}\right)+N_2\sin\left(\frac{\pi}{2}\right). \quad (18)$$

To compare the results, the calculation is carried out at a constant value of the stiffness coefficient of the joint k_u. According to [14] for bolted joints with toothed connectors, this coefficient is determined by the formula:

$$k_u=\frac{2}{3}k_{ser}, \quad (19)$$

where k_{ser} is normative coefficient of connectors stiffness, defined as a secant modulus at a load equal to 40 % of the maximum allowable value.

3. Results and Discussion

Forces in shear bonds at all loading stages, total applied values of longitudinal forces and predicted values of critical force are presented in Tables 1–3. At the 14th step of the calculation, the accuracy indicator for determining the critical force was less than 1 %, so the pillar was not loaded further.

Table 1. Calculation progress (stages 1-5).

Bond number	Calculation stage number, *m*														
	1			2			3			4			5		
	c, kN/m	ΔT, kN	$\sum T$, kN	c, kN/m	ΔT, kN	$\sum T$, kN	c, kN/m	ΔT, kN	$\sum T$, kN	c, kN/m	ΔT, kN	$\sum T$, kN	c, kN/m	ΔT, kN	$\sum T$, kN
1,1 (2,1)	56016	4.89	4.89	49807	4.67	9.57	39529	4.22	13.79	28976	3.63	17.42	20554	3.01	20.43
1,2 (2,2)	56016	2.02	2.02	54227	2.12	4.14	51148	2.33	6.47	46672	2.57	9.03	40823	2.74	11.77
1,3 (2,3)	56016	0.83	0.83	55431	0.90	1.72	54563	1.03	2.75	53285	1.23	3.98	51419	1.46	5.44
1,4 (2,4)	56016	0.33	0.33	55807	0.36	0.70	55538	0.42	1.12	55174	0.51	1.63	54662	0.63	2.26
1,5 (2,5)	56016	0.12	0.12	55947	0.13	0.25	55865	0.15	0.40	55764	0.18	0.58	55630	0.23	0.81
ΔN, kN	50			50			50			50			50		
$\sum N$, kN	50			100			150			200			250		
$\sum N_{cr}$, kN	863.23			862.16			860.49			857.95			854.05		
Δ, %	–			–			–			–			–		

Table 2. Calculation progress (stages 6–10).

Bond number	Calculation stage number, *m*														
	6			7			8			9			10		
	c, kN/m	ΔT, kN	$\sum T$, kN	c, kN/m	ΔT, kN	$\sum T$, kN	c, kN/m	ΔT, kN	$\sum T$, kN	c, kN/m	ΔT, kN	$\sum T$, kN	c, kN/m	ΔT, kN	$\sum T$, kN
1,1 (2,1)	14971	2.51	22.94	11800	2.20	25.14	10325	2.08	27.22	9989	2.12	29.34	10264	2.25	31.58
1,2 (2,2)	34038	2.75	14.51	27197	2.58	17.10	21236	2.30	19.40	16687	1.99	21.39	13574	1.74	23.12
1,3 (2,3)	48771	1.70	7.14	45224	1.90	9.03	40826	2.02	11.05	35852	2.02	13.07	30763	1.93	15.00
1,4 (2,4)	53930	0.77	3.03	52889	0.91	3.94	51487	1.05	4.99	49626	1.18	6.17	47304	1.27	7.43
1,5 (2,5)	55451	0.28	1.08	55208	0.34	1.42	54884	0.40	1.82	54458	0.46	2.28	53913	0.51	2.79
ΔN, kN	50			50			50			50			50		
$\sum N$, kN	300			350			400			450			500		
$\sum N_{cr}$, kN	848.26			840.02			829.05			815.23			798.95		
Δ, %	–			–			–			–			–		

Table 3. Calculation progress (stages 11–14).

Bond number	Calculation stage number, m											
	11			12			13			14		
	c, kN/m	ΔT, kN	$\sum T$, kN	c, kN/m	ΔT, kN	$\sum T$, kN	c, kN/m	ΔT, kN	$\sum T$, kN	c, kN/m	ΔT, kN	$\sum T$, kN
1,1 (2,1)	10001	2.27	33.85	6424	1.66	35.52	1188	0.38	35.89	1081	0.35	36.24
1,2 (2,2)	11624	1.59	24.71	10513	1.67	26.39	10017	1.99	28.37	10112	2.08	30.46
1,3 (2,3)	26016	1.82	16.82	21830	1.84	18.67	18031	1.97	20.64	14643	1.72	22.36
1,4 (2,4)	44561	1.35	8.78	41423	1.55	10.33	37639	1.87	12.20	32942	1.82	14.03
1,5 (2,5)	53236	0.58	3.37	52395	0.70	4.07	51264	0.92	4.99	49623	1.00	6.00
ΔN, kN	50			50			50			50		
$\sum N$, kN	550			600			650			700		
$\sum N_{cr}$, kN	779.95			755.22			719.12			704.27		
Δ, %	–			25.87			10.64			0.61		

Fig. 6, a shows graphs of the increase in shear forces in shear bonds as the considered pillar is loaded with load steps ΔN. Graphs of force changes in bonds T_1 and T_2 are concave inward, and T_3, T_4 and T_5 are outward. From which it follows that from stage to stage of loading, the forces are redistributed between the bonds located closer to the end sections of the element and located closer to the axis of symmetry (cross section with zero shear). As whole, it can judge that the stiffness coefficient of more loaded bonds near the end sections decreases faster than that of bonds in the middle section, which negatively affects the operation of the entire structure with each stage of loading, reducing the predicted value of the critical force by an increasing value.

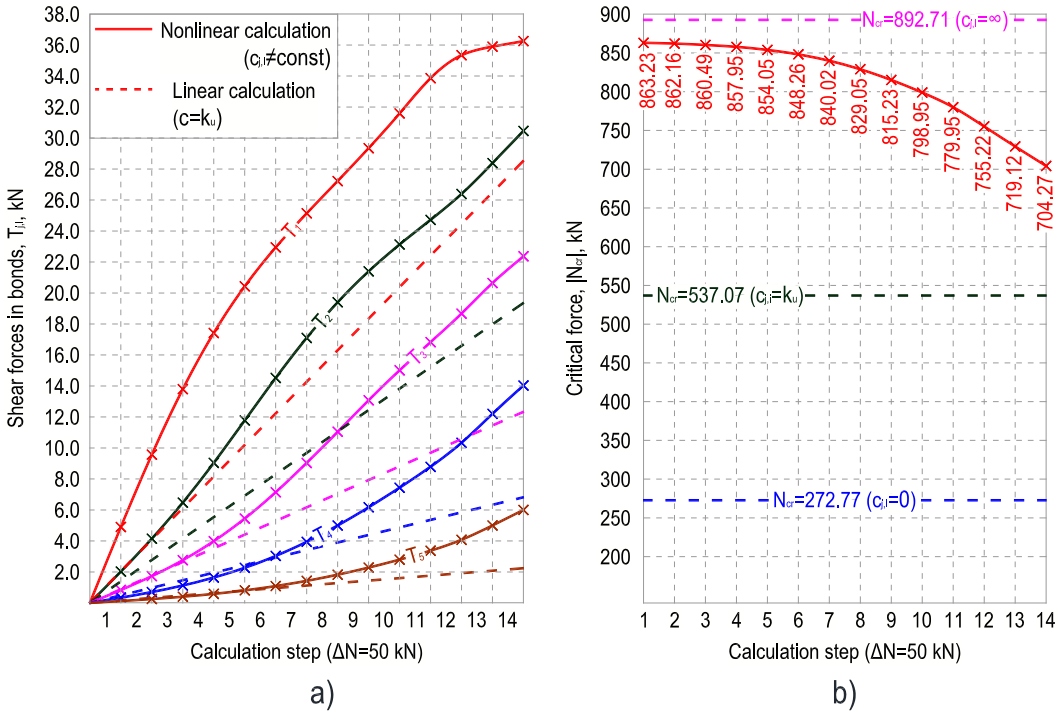

Figure 6. Dependency graphs: *a* – forces in shear bonds T_i at each stage of the calculation; *b* – critical force values in nonlinear calculation (predicted value at each step) and linear calculation for various values of the stiffness coefficient of the connectors *c*; N_{cr} ($c = \infty$) is the critical force for solid section rod; N_{cr} ($c = k_u$) is the same, for composite rod with normative coefficient of connectors stiffness k_u (19); N_{cr} ($c = 0$) is the same, for composite rod without shear connectors.

The paper [23] presents the results of the study of the stress–strain state of square concrete-filled double-skin steel tubular columns under axial compression taking into account the physical nonlinearity of deformation of materials. A new design equation is suggested based on stress distribution over the concrete cross-section. It is shown that material properties and dimensions of composite columns can highly affect their performance. Also, the thickness of the inner tube must be controlled to prevent its premature failure. In the article [24], the supercritical forms of buckling loss of hyperelastic columns under axial compression are investigated. As its width-to-length ratio increases, the column can undergo transitions from continuous buckling, like the Euler buckling, to snapping-through buckling, and eventually to snapping-back buckling. The results of these studies give reason to believe that taking into account the physical and geometric nonlinearity makes it possible to identify a noticeable error in the assessment of buckling compared to the calculation according to an undeformed scheme under the assumption of linear work of materials.

In the process of searching for sources, it was not possible to find works related to the buckling of composite structures with nonlinear deformable connections, however, the results of this study gives grounds to judge that the actual reserves of the bearing capacity and stability of such structures can be adequately obtained only with a nonlinear calculation and a sufficient number of iterations. In the linear calculation of such a pillar, an erroneous decision can be adopted about the need to increase the number of bonds near the end sections, or reduce their spacing, although in reality such a need does not arise. When taking into account the “normative” stiffness coefficient of the bonds, the forces in them do not exceed 80 % of the maximum permissible value, however, in this case, a significantly underestimated (in the case under consideration by 24 %) value of the critical load is obtained. Depending on the character of the deformation curve of the shear connectors and the bending stiffnes flexibility of the element layers, the calculation using the normative linear stiffness coefficient (19) may also leads to overestimated values of the critical force N_{cr}, since the actual stiffness of the connectors depends on the shear forces level in the moment of buckling, which are significantly different for rods with high and low flexibility of layers.

The actual reserve of the bearing capacity of centrally compressed component columns with nonlinearly deformable shear bonds is almost impossible to predict in advance, but it will be between two values of the critical load: calculated for a solid element (at $c_{j,i} \to \infty$) and for a composite element, taking into account zero stiffness seams $\left(c_{j,i} \to 0 \right)$. These values can be used when assigning the value of the load step, on which the number of iterations will depend. To obtain adequate values, the number of iterations should be 10...15 [25].

The use of the presented calculation algorithm can be extended to component elements with defects, the nature of which causes the variability of the geometric characteristics of the rod sections along the length (for example, a wooden pillar with longitudinal cracks); component structures with disconnected bonds (when calculating according to the idealized Prandtl diagram); as well as structures, the material of which creates the need to calculate them taking into account the physical nonlinearity. The introduction of an additional variable, the time factor, allows to consider the influence of creep deformations of joints in the calculation.

4. Conclusions

1. A mathematical model has been devised that makes it possible to calculate the strength and stability of three-layer compressed component rods, taking into account the nonlinear operation of shear bonds; with an uneven arrangement of bonds; when using idealized bond deformation diagrams, described, for example, according to the Prandtl diagram.

2. When taking into account the “normative” stiffness coefficient of the bonds, the forces in them do not exceed 80 % of the maximum permissible value, however, in this case, a significantly underestimated (in the case under consideration by 24 %) value of the critical load is obtained.

3. The introduction of the normative coefficient of connections stiffness into the calculation may give an invalid value of the critical force and does not allow obtaining reliable values of shear forces in the bonds, taking into account redistribution. A correct bucking estimation of the such structures should be produced taking into account the uneven stiffness coefficient changes of shear connections according to actual deformation curves.

References

1. Jockwer, R., Grönquist, P., Frangi, A. Long-term deformation behaviour of timber columns: Monitoring of a tall timber building in Switzerland. Engineering Structures. 2021. 234. 111855. DOI: 10.1016/j.engstruct.2021.111855

2. Kia, L., Valipour, H.R. Composite timber-steel encased columns subjected to concentric loading. Engineering Structures. 2012. 232. 111825. DOI: 10.1016/j.engstruct.2020.111825
3. Qiao, Q., Yang, Z., Mou, B. Experimental study on axial compressive behavior of CFRP confined square timber filled steel tube stub columns. Structures, 2020. 24. Pp. 823–834. DOI: 10.1016/j.istruc.2020.02.007
4. Navaratnam, S., Thamboo, J., Poologanathan, K., Roy, K., Gatheeshgar, P. Finite element modelling of timber infilled steel tubular short columns under axial compression. Structures. 2021. 30. Pp. 910–924. DOI: 10.1016/j.istruc.2020.12.087
5. Karampour, H., Bourges, M., Gilbert, B.P., Bismire, A., Bailleres, H., Guan, H. Compressive behaviour of novel timber-filled steel tubular (TFST) columns. Construction and Building Materials. 2020. 238. 117734. DOI: 10.1016/j.conbuildmat.2019.117734
6. Ghanbari-Ghazijahani, T., Magsi, G.A., Gu, D., Nabati, A., Ng, C.T. Double-skin concrete-timber-filled steel columns under compression. Engineering Structures. 2019. 200. 109537. DOI: 10.1016/j.engstruct.2019.109537
7. Hu, Q., Gao, Y., Meng, X., Diao, Y. Axial compression of steel–timber composite column consisting of H-shaped steel and glulam. Engineering Structures. 2020. 216. 110561. DOI: 10.1016/j.engstruct.2020.110561
8. Xu, F., Xuan, S., Li, W., Meng, X., Gao, Y. Compressive performance of steel-timber composite L-shaped columns under concentric loading. Journal of Building Engineering. 2022. 48. 103967. DOI: 10.1016/j.jobe.2021.103967
9. Li, H., Qiu, H., Lu, Y. An analytical model for the loading capacity of splice-retrofitted slender timber columns. Engineering Structures. 2020. 225. 111274. DOI: 10.1016/j.engstruct.2020.111274
10. Bhat, J.A. Buckling behavior of cross laminated poplar timber columns using various performance improvement techniques. Materials Today: Proceedings. 2021. 44. Pp. 2792–2796. DOI: 10.1016/j.matpr.2020.12.785
11. Wei, P., Wang, B.J., Li, H., Wang, L., Peng, S., Zhang, L. A comparative study of compression behaviors of cross-laminated timber and glued-laminated timber columns. Construction and Building Materials. 2019. 222. Pp. 86–95. DOI: 10.1016/j.conbuildmat.2019.06.139
12. Rimshin, V.I., Labudin, B.V., Melekhov, V.I., Orlov, A.O., Kurbatov, V.L. Improvement of strength and stiffness of components of main struts with foundation in wooden frame buildings. ARPN Journal of Engineering and Applied Sciences. 2018. 13(11). Pp. 3851–3856.
13. Rimshin, V., Labudin, B., Morozov, V., Orlov, A., Kazarian, A., Kazaryan, V. Calculation of Shear Stability of Conjugation of the Main Pillars with the Foundation in Wooden Frame Buildings. International Scientific Conference Energy Management of Municipal Facilities and Sustainable Energy Technologies EMMFT 2018. 2019. Pp. 867–876. Springer International Publishing.
14. CEN EN 1995−1−1:2004/A2−2014 Eurocode 5: Design of timber structures − Part 1−1: General − Common rules and rules for buildings.
15. Šmak, M., Straka, B. Development of new types of timber structures based on theoretical analysis and their real behaviour. Wood Research. 2014. 59(3). Pp. 459–470.
16. Lokaj, A., Klajmonová, K. Round timber bolted joints exposed to static and dynamic loading. Wood Research. 2014. 59(3). Pp. 439–448.
17. Karelskiy, A.V., Zhuravleva, T.P., Labudin, B.V. Load-to-failure bending test of wood composite beams connected by gang nail. Magazine of Civil Engineering. 2015. 54(2). Pp. 77–85. DOI: 10.5862/MCE.54.9
18. Chernykh, A., Danilov, E., Koval, P. Stiffness Analysis of Connections of LVL Structures with Claw Washers. Lesnoy Zhurnal (Forestry Journal). 2020. 4. Pp. 157–167. DOI: 10.37482/0536-1036-2020-4-157-167
19. Baszeń, M. Semi-rigid Behavior of Joints in Wood Light-frame Structures. Procedia Engineering. 2017. 172. Pp. 88–95. DOI: 10.1016/j.proeng.2017.02.022
20. Hassanieh, A., Valipour, H. Experimental and numerical study of OSB sheathed-LVL stud wall with stapled connections. Construction and Building Materials. 2020. 233. 117373. DOI: 10.1016/j.conbuildmat.2019.117373
21. Labudin, B.V., Popov, E.V., Vladimirova, O.A., Sopilov, V.V., Bobyleva, A.V. Wood-Composite Structures with Non-Linear Behavior of Semi-Rigid Shear Ties. Construction of Unique Buildings and Structures. 2021. 97. 9702. DOI: 10.4123/CUBS.97.2
22. Popov, E.V., Sopilov, V.V., Bardin, I.N., Lyapin, D.M. (2021). Calculation of Vertical Deformations of Composite Bending Wooden Structures with Non-linear Behavior of Shear Bonds. Environmental and Construction Engineering: Reality and the Future. Pp. 109–116. Springer International Publishing.
23. Ayough, P., Ramli Sulong, N.H., Ibrahim, Z., Hsiao, P.C. Nonlinear analysis of square concrete-filled double-skin steel tubular columns under axial compression. Engineering Structures. 2020. 216. 110678. DOI: 10.1016/j.engstruct.2020.110678
24. Chen, Y., Jin, L. From continuous to snapping-back buckling: A post-buckling analysis for hyperelastic columns under axial compression. International Journal of Non-Linear Mechanics. 2020. 125. 103532. DOI: 10.1016/j.ijnonlinmec.2020.103532
25. Popov, E.V., Karelsky, A.V., Sopilov, V.V., Labudin, B.V., Cherednichenko, V.V. Calculation features of compressed-bent build-up timber columns with nonlinear-deformable shear bracings. IOP Conference Series: Materials Science and Engineering. 2022. 1211(1). 012007. DOI: 10.1088/1757-899x/1211/1/012007

Information about author:

Egor Popov, *PhD in Technical Sciences*
ORCID: https://orcid.org/0000-0002-8950-7558
E-mail: EPV1989@yandex.ru

Boris Labudin, *Doctor of Technical Sciences*
ORCID: https://orcid.org/0000-0002-2547-3096
E-mail: sevned@mail.ru

Anatolij Konovalov, *PhD in Technical Sciences*

ORCID: https://orcid.org/0000-0003-2810-6336
E-mail: a.konovalov@narfu.ru

Alexander Karelskiy,
E-mail: kaw_79@mail.ru

Valerii Sopilov,
ORCID: https://orcid.org/0000-0002-1236-5950
E-mail: sopilov.v@edu.narfu.ru

Aleksandra Bobyleva,
ORCID: https://orcid.org/0000-0002-1216-7567
E-mail: aleksandra-bobyleva@mail.ru

Denis Stolypin,
ORCID: https://orcid.org/0000-0003-0153-8729
E-mail: Stolypin.Denis.A@yandex.ru

Received 12.05.2022. Approved after reviewing 17.01.2023. Accepted 17.01.2023.